Towards a Molecular Basis for Understanding the Behavior of Isotopic Polymer Blends: Lattice Cluster Theory Computations for PSD/PSH Blends

Jacek Dudowicz, Karl F. Freed,* and Masha Lifschitz

The James Franck Institute and the Department of Chemistry, University of Chicago, Chicago, Illinois 60637

Received March 7, 1994; Revised Manuscript Received June 25, 1994®

ABSTRACT: The binary blend lattice cluster theory (LCT) is applied to isotopic polystyrene (PSD/PSH) blends to study the combined influence on blend physical properties of local correlations, monomer molecular structure, and blend compressibility, as well as of asymmetries in interactions, molecular weights, and monomer structures. The LCT computations of the small-angle neutron scattering effective interaction parameter χ_{eff}, the coexistence curve, and the interfacial profile in phase-separated PSD/PSH blends provide good agreement with experimental data, indicating internal consistency. The computations do not yield the parabolic upward composition dependence of χ_{eff} that is observed for isotopic blends of polybutadienes and polyethylenes. We speculate that this upward behavior arises from the random copolymer nature of these systems.

I. Introduction

One phenomenon that most exemplifies the subtlety of phase behavior in polymer systems involves the observed phase separation between isotopic blends which are mixtures of hydrogenated and perdeuterated polymers of the same chemical species. The appearance in these isotopic blends of critical temperatures in excess of room temperatures illustrates the fact that the relevant monomer–monomer interaction energies determining phase separation in polymer blends are on the order of $10^{-3}k_BT$ per monomer, where k_BT is the thermal energy. Thus, no available molecular mechanics or quantum mechanical methods are of sufficient accuracy to provide ab initio predictions of these critical temperatures, and the only possible descriptions of this phase separation require the use of approximate phenomenological models. The subtle differences between the hydrogenated and perdeuterated isotopomers focus attention on ascertaining the salient physical mechanisms leading to the phase separation as well as to other observed physical properties of these systems.

Experiments have been performed for isotopic blends of polybutadienes (PB), polystyrenes (PS), and polyethylenes (PE) with somewhat different properties exhibited. The majority of experiments involve measurements of the small-angle neutron scattering in which extrapolation to zero angle and analysis with the incompressible random-phase approximation[1] (IRPA) lead to the determination of an effective Flory interaction parameter χ_{eff}. The experiments for PSD/PSH blends display χ_{eff} as a concave function of composition,[2,3] while χ_{eff} for the other two systems is found to be convex.[2,4] Data for PSD/PSH by Bates and co-workers[2] differ somewhat from those of Schwahn and co-workers,[3] who find negative χ_{eff} for high or low PSD compositions. Thus, Bates and co-workers[2] have raised the question of how it is possible for a system with inherently repulsive interactions to exhibit a negative χ_{eff} at any blend composition. A possible resolution of this particular point is already suggested by our previous paper[5] that includes "equation of state effects" (also called "compressibility") to demonstrate the possible emergence of such negative χ_{eff} behavior from small-angle neutron scattering as arising solely due to the fact that these blends are not completely incompressible. Hence, an artificial consequence of using the IRPA definition is the mistaken interpretation of χ_{eff} as a (dimensionless) microscopic interaction energy.

More fundamental questions, however, are associated with the observation of concave and convex composition dependences of χ_{eff} for different isotopic blends.[2-4] This finding is important by its indication that the physical origins of the isotopic D/H blend phase separation may not be governed by a single universal mechanism. Several theoretical computations in the literature claim to be in qualitative agreement with some or all of the experimental data for the χ_{eff} of the isotopic blends. However, it is clear that all computations, using discrete or continuum space potentials, are based on oversimplified models that contain some but not all essential features of the differences between the H and D isotopomers.

Many of the theoretical discussions of isotopic blends follow the arguments of Bates and co-workers[6] that the isotopic blends must be systems with negligible entropic contributions to χ_{eff} because of the otherwise identity of the isotopomers. Consequently, this model implies that the main differences appear because of energetic asymmetries between the H- and D-containing monomers. Bates and co-workers[6] ascribe these departures as arising from different monomer volumes (due to disparate zero point vibrations) and polarizabilities of the two isotopic species. It also assumed[6] that the volumes and polarizabilities for a given isotope are proportional to each other for the hydrogenated polyolefins. Thus, if α_H is the polarizability of the hydrogen-containing monomer and ϵ_{HH} is the van der Waals attractive interaction energy between pairs of hydrogenated monomers, this "polarizability model" implies that $\epsilon_{HH} \propto (\alpha_H)^2$, and hence we likewise have $\epsilon_{DD} \propto (\alpha_D)^2$ and $\epsilon_{HD} = (\epsilon_{HH}\epsilon_{DD})^{1/2} \propto \alpha_H\alpha_D$. It then follows from the IRPA that χ_{eff} for the isotopic blend is proportional to the positive quantity $(\alpha_H - \alpha_D)^2$. The occurrence of a positive χ_{eff} is consistent with the appearance of an upper critical solution temperature (UCST). On the other hand, lattice cluster computations of Bawendi and Freed[7] indicate that a small but nonzero entropic contribution to χ_{eff} emerges even for blends of identical species provided they have different polymerization indices, while Curro and Schweizer[8] use a continuum thread model to explain how different monomer volumes for the isotopic species

® Abstract published in *Advance ACS Abstracts*, August 1, 1994.

0024-9297/94/2227-5387$04.50/0

lead to a size asymmetry which also induces an entropic contribution to χ_{eff} for the blend. These theoretical considerations are in accord with the presence of a nonnegligible entropic contribution to the observed χ_{eff} of isotopic blends,[2-4] but they question explanations which ascribe the isotopic blend χ_{eff} solely to polarizability (and the equivalent volume) differences. In summary, theoretical arguments point to a possible combination of energetic, size, and molecular weight asymmetries in concert with equation of state effects as providing the subtle mechanism for the differing behaviors of the composition variation in χ_{eff} for isotopic blends.

We apply lattice cluster theory[9,10] (LCT) to isotopic blends along with new theoretical treatments[11,12] of interfacial profiles for phase-separated compressible polymer blends. The lattice cluster theory[10] is based on a generalized lattice model, which enables the description of the combined influences of monomer molecular structure, local correlations, and equation of state effects. Our previous studies[13] with the LCT emphasize the importance of considering both an adequate molecular theory and a variety of different experimental measurements in any attempt to extract meaningful *microscopic* information about polymer blends. Thus, we choose to analyze in detail the isotopic blend PSD/PSH for which the most extensive set of experimental data is available. These data include the composition and temperature dependence of χ_{eff} from small-angle neutron scattering[2,3] and both the coexistence curve[14] and the interfacial profile[14] in phase-separated blends. Prior computations[13,15,16] with the lattice cluster theory[10] indicate the important combined influences of monomer molecular structures, local correlations, and compressibility in determining the composition dependence of both the entropic and enthalpic portions of the small-angle neutron scattering χ_{eff}. Furthermore, as noted above, the inclusion of equation of state effects allows the prediction, in principle, of negative χ_{eff} at high and low PSD compositions, despite the existence of a positive microscopic interaction energy parameter for a hypothetical incompressible blend. Hence, the use of the lattice cluster theory enables probing reasons for the different behaviors[2,3] observed by Bates and Schwahn and their respective co-workers. One deficiency of the generalized lattice model, however, lies in its inability to describe size asymmetries between the isotopomers. Thus, results obtained by Curro and Schweizer[8] for the continuum thread model are used to append into our LCT computations entropic contributions to χ_{eff} from this size asymmetry in order to investigate the composition dependence of χ_{eff} for the PE isotopic blend, the system most closely corresponding to the Curro–Schweizer model.

In comparing lattice cluster theory predictions and experimental data, it must be borne in mind that the theory is based upon an admittedly oversimplified lattice model. Various limitations are inherent in any lattice model, and the present computations deviate from full "reality" in their use of a cubic lattice, the neglect of semiflexibility, the use of nearest-neighbor interactions, and the consideration of simplified monomer structures. Nevertheless, the theory provides a description of the gross influences on thermodynamic properties of monomer shapes, local correlations, and equation of state effects. Are these qualitative descriptions adequate to describe the detailed behavior of "real" systems? The answer to this important question is far from obvious and can only emerge from using the lattice cluster theory predictions as a phenomenological model to be compared to the most extensive possible sets of experimental data. If, for instance, the observed χ_{eff} data for the PSD/PSH blend are merely most sensitive to general interaction and molecular weight asymmetries, overall monomer sizes and shapes, local packing and interaction induced correlations, and equation of state effects, then there is a reasonable expectation that the phenomenological use of the simple lattice model is sufficient to describe the observed behavior of these isotopic blends. If, however, the behavior arises from subtle details of the actual potentials, the lattice model would be inadequate, and improved theories would be required. The improved theories might be constructed by further developments of the lattice cluster theory to incorporate more aspects of reality, or they could require use of much more sophisticated atomistic nonlattice theories. The latter approaches would necessitate very heavy numerical computations, especially for the coexistence curves, and they are to be contrasted with the almost trivial computational requirements for applications of the analytical formulas of the lattice cluster theory.

Our use here of the lattice cluster theory free energy expressions as a phenomenological model follows in the long-standing tradition of using Flory–Huggins, Guggenheim, and equation of state theories as the basis of phenomenological descriptions of real polymer blends. The lattice cluster theory, however, is a more complete solution of a more realistic generalized lattice model, but the rigor of the theoretical treatment, perhaps, makes more apparent the departures of this improved model from ultimate reality. Our applications of the lattice cluster theory to PSD/PSH blends, therefore, are designed to probe the limitations of the lattice cluster theory as a guide to future efforts for rectifying these limitations, to determine the qualitative features governing the thermodynamic properties of these systems, and to aid in sorting out some of the puzzling data in the literature for these isotopic blends.

Section II outlines the theoretical background by briefly describing how the effective interaction parameter χ_{eff}, the coexistence curve, and the interfacial profile in isotopic polymer blends are evaluated from the lattice cluster theory. Our recent theory[11] of interfacial profiles for compressible blends is generalized here to asymmetric blends in order to compute the PSD/PSH interfacial profile. A future paper[12] will provide a complete derivation and technical details of this theoretical extension, which applies to blends with molecular weight, monomer structure, and interaction asymmetries. The LCT computations of χ_{eff}, the coexistence curve, and the interfacial profile for PSD/PSH blends are described in section III which also presents a direct comparison of these calculated properties with experimental data. Section IV analyzes available SANS data for χ_{eff} of the other isotopic blends as well as the theoretical calculations[17] and computer simulations[18-20] which are quoted in the literature as supporting these observations. This analysis is designed to understand factors influencing the composition dependence of χ_{eff} for these systems.

II. Lattice Cluster Theory of a Binary Blend

A. Model of an Isotopic Blend. The extended lattice model of a binary blend represents each component α (α = 1 and 2) as n_α monodisperse polymer chains placed on a regular array of N_l lattice sites and coordination number z^*. A single chain of species α occupies $M_\alpha = N_\alpha s_\alpha$ lattice sites, where N_α is the polymerization index and s_α designates the number of lattice sites covered by a single monomer of species α. The latter quantity reflects the monomer's internal architecture and size, subject to the

limitations imposed by the lattice morphology. The monomer structure is chosen, whenever possible, as most closely corresponding to a united atom model in which united atom groups, such as CH_n, reside at single lattice sites. However, differences in sizes between CH_n and CD_n groups cannot be represented by such a lattice model. Hence, the same monomer structure is prescribed for both components of an isotopic blend, and the monomer occupancy indices s_1 and s_2 are equal to each other. This implies that the blend noncombinatorial entropy may arise only from the difference in polymerization indices N_1 and N_2, if any, or from equation of state effects. Blend compressibility implies the existence of excess free volume which is modeled by the presence of n_v empty sites (voids) with volume fraction $\phi_v = n_v/N_1$. The void volume fraction ϕ_v is determined from the equation of state, and all quantites are evaluated at a pressure of 1 atm or 10^{-5} Torr. The composition of the compressible binary blend is expressed below in terms of the actual volume fractions $\phi_\alpha = n_\alpha M_\alpha/N_1$ (normalized as $\phi_1 + \phi_2 + \phi_v = 1$) or of the nominal volume fractions $\Phi_1 = 1 - \Phi_2 = \phi_1/(1 - \phi_v)$, and the lattice is assumed to be a three-dimensional cubic lattice with $z^* = 6$.

Generally, interactions in fluids involve short-range repulsions and longer range attractions. While the former are naturally represented in the lattice model by excluded-volume constraints, the latter are introduced by ascribing the attractive microscopic van der Waals energy $\epsilon_{\alpha\beta}^{i,j}$ to nearest-neighbor (on the lattice) portions i and j of monomers α and β. For simplicity, all s_α portions of a monomer α are taken as energetically equivalent units, which interact with the same energy $\epsilon_{\alpha\beta}$. This simplification leads for a compressible system to the presence of three independent interaction energies ϵ_{11}, ϵ_{22}, and ϵ_{12}. It is possible to permit different portions of the monomer to interact with different group-specific interactions, but this would lead to the introduction of additional parameters, something to be avoided until warranted by experimental data.

B. Free Energy of a Binary Blend. The lattice cluster theory[9,10] (LCT) represents the Helmholtz free energy F of a binary blend in the form

$$\frac{F}{N_1 k_B T} = \phi_v \ln \phi_v + \sum_{i=1}^{i=2} \frac{\phi_i}{M_i} \ln \frac{2\phi_i}{M_i} - (\ln z^* - 1) \sum_{i=1}^{i=2} \left(1 - \frac{1}{M_i}\right) \phi_i + \sum_{k=1}^{k^*} \sum_{l=0}^{k} f_{kl} \phi_1^{\,l} \phi_2^{\,k-l} \quad (2.1)$$

where the last term on the right-hand side of eq 2.1 provides the noncombinatorial part of F. A series of our papers[9,10,15] describes the method for generating the coefficients f_{kl} in eq 2.1 and tabulates the corrections to the usual Flory–Huggins theory that arise from local correlations and monomer structure. These coefficients are obtained from the LCT as double expansions in the inverse lattice coordination number $1/z^*$ and in the three dimensionless microscopic van der Waals attractive energies $\epsilon_{\alpha\beta}/k_BT$. The coefficients in these double expansions depend on the monomer structures of the two blend components and on the occupancy indices M_1 and M_2. Only terms through orders $1/(z^*)^2$ and $(\epsilon_{\alpha\beta}/k_BT)^2$ are retained in the present calculations of F. This approximation fixes[10] the upper limit of k in the double summation in eq 2.1 as $k^* = 6$.

Experiments at constant pressure are most appropriately described by the Gibbs free energy G

$$G = F + PV = F + PN_1 v_{cell} \quad (2.2)$$

where the pressure P is computed as

$$P \equiv -\left.\frac{\partial F}{\partial V}\right|_{T,n_1,n_2} = -\left.\frac{1}{v_{cell}} \frac{\partial F}{\partial n_v}\right|_{T,n_1,n_2} \quad (2.3)$$

The volume v_{cell} associated with one lattice site is assumed to be constant and is estimated from the monomer volumes v_α and monomer occupancy indices s_α as

$$v_{cell} = \frac{(v_1 v_2)^{1/2}}{(s_1 s_2)^{1/2}} \quad (2.4)$$

The equation of state derived from eq 2.3 is used to determine ϕ_v for given P, T, and Φ_1.

C. Small-Angle Neutron Scattering Effective Interaction Parameter χ_{eff}. The small-angle neutron scattering effective Flory interaction parameter is a central quantity in any theory of polymer fluids. For our extended lattice model of isotopic binary blends, χ_{eff} is defined as

$$\chi_{eff} = -\frac{1}{2}\left[\frac{1}{S(0)} - \frac{1}{M_1\Phi_1} - \frac{1}{M_2\Phi_2}\right] \quad (2.5)$$

where $S(0)$ represents the extrapolated zero-angle neutron scattering function, the M_α denote individual chain occupancy indices, and the Φ_α designate the nominal volume fractions which satisfy the condition $\Phi_1 + \Phi_2 = 1$. The total extrapolated zero-angle structure factor $S(0)$ in eq 2.5 is, in general, a weighted sum of the zero wave vector partial structure factors $S_{\alpha\beta}(0)$,

$$S(0) = p_1^{\,2} S_{11}(0) + 2p_1 p_2 S_{12}(0) + p_2^{\,2} S_{22}(0) \quad (2.6)$$

where the weights p_1 and p_2 are reduced scattering lengths that are normalized such that $p_1 - p_2 = 1$. When the scattering contrast is complete (i.e., only monomers of one species, say species 1, scatter), the reduced scattering length for species 2 vanishes ($p_2 = 0$) and eq 2.6 simplifies to

$$S(0) = S_{11}(0) \quad (2.7)$$

The zero wave vector partial structure factors $S_{\alpha\beta}(0)$ are related to the chemical potentials μ_1 and μ_2 by

$$S_{\alpha\beta}(0)^{-1} = \frac{N_1}{M_\alpha M_\beta k_B T} \left.\frac{\partial \mu_\alpha}{\partial n_\beta}\right|_{T,V,\mu_\beta} \quad (2.8)$$

The chemical potentials μ_1 and μ_2, in turn, are calculated from the free energy (2.1) as

$$\mu_\alpha = \left.\frac{\partial F}{\partial n_\alpha}\right|_{T,V,n_\beta} \quad (2.9)$$

where the volume V in eq 2.9 is evaluated from the equation of state in order to have a proper comparison with experiments at constant pressure. Hence, the use of the LCT free energy F and eqs 2.3–2.9 enables us to determine the effective interaction parameter (2.5) from the lattice cluster theory. The χ_{eff} in eq 2.5 is, however, a dimensionless quantity, normalized to a pair of lattice sites, while experimentalists employ somewhat different definitions χ'_{eff} or Γ as is now explained.

The experimental neutron scattering data for isotopic blends are generally analyzed in terms of either a dimensionless monomer–monomer interaction parameter[2,4] χ'_{eff},

$$\chi'_{eff} = -\frac{1}{2}\left[\frac{1}{S'(0)} - \frac{1}{N_1\Phi_1} - \frac{1}{N_2\Phi_2}\right] \quad (2.10)$$

or dimensional generalized interaction parameter[3] Γ,

$$\Gamma = -\frac{1}{2}\left[\frac{1}{I(0)} - \frac{1}{\Phi_1\Phi_2\bar{V}}\right] \tag{2.11}$$

having units of mol/cm^3. The total scattering intensity $I(0)$ in eq 2.11 and the scattering structure factor $S'(0)$ in eq 2.10 are related to each other by

$$I(0) = S'(0)\frac{V_1v_2 + V_2v_1}{V_1\Phi_1 + V_2\Phi_2} \tag{2.12}$$

where V_α and v_α are chain and monomer volumes for species α, respectively. The average chain volume $\bar{V}$ in eq 2.11 is given by

$$\bar{V} = \frac{V_1V_2}{V_1\Phi_1 + V_2\Phi_2} \tag{2.13}$$

A simple analysis of eqs 2.5, 2.10, and 2.11 leads to the interelations between χ_{eff}, χ'_{eff}, and Γ as

$$\chi_{eff} = \chi'_{eff}/s, \quad \text{for } s \equiv s_1 = s_2 \tag{2.14}$$

and

$$\chi_{eff} = \Gamma\bar{V}/\bar{M} \tag{2.15}$$

with $\bar{M} \equiv M_1M_2/(M_1\Phi_1 + M_2\Phi_2)$ being the analog of eq 2.13. Equations 2.14 and 2.15 are used in section III to convert between the different definitions and to enable comparison of the computed LCT effective interaction parameters χ_{eff} with experimental data for PSD/PSH blends.

D. Coexistence Curves and Interfacial Profiles. A binary polymer blend can form a homogeneous phase or a two-phase system. When phase separation occurs at constant pressure P, the coexisting phases (designated as I and II) have equal pressures and equal chemical potentials for both blend components,

$$\mu_\alpha^{(I)} = \mu_\alpha^{(II)}, \quad \alpha = 1 \text{ and } 2 \tag{2.16}$$

$$P^{(I)} = P, \quad P^{(II)} = P$$

The binary blend coexistence phase is described by the set of data points $\{T, \phi_1^{(I)}, \phi_2^{(I)}, \phi_1^{(II)}, \phi_2^{(II)}\}$ (or equivalently by $\{T, \Phi_1^{(I)}, \phi_v^{(I)}, \Phi_1^{(II)}, \phi_v^{(II)}\}$) that satisfies eqs 2.16.

Since the interfacial profile experiments by Klein and co-workers[14] involve a planar interface, we specialize the theory[11] of interfacial properties to planar interfaces (perpendicular to the z axis) and compressible binary blends. Given two coexisting phases at constant temperature and pressure, the compositions $\phi_1 = \phi_1(z)$ and $\phi_2 = \phi_2(z)$ of both components vary through the planar interface. The total free energy functional $\mathbf{F}$ for a phase-separated system is expressed as the sum of homogeneous and inhomogeneous contributions,

$$\mathbf{F} = \mathbf{F}_h + \mathbf{F}_{inh} \tag{2.17}$$

The inhomogeneous $\mathbf{F}_{inh}$ portion of the functional $\mathbf{F}$ is given by

$$\mathbf{F}_{inh} = \frac{1}{36}\int_{-\infty}^{\infty}dz\left[\frac{l_1^2}{s_1\phi_1}\left(\frac{d\phi_1}{dz}\right)^2 + \frac{l_2^2}{s_2\phi_2}\left(\frac{d\phi_2}{dz}\right)^2\right] \tag{2.18}$$

where l_α and s_α are respectively the Kuhn length and monomer occupancy index for species α. Equation 2.18 has been derived by Tang and Freed[21] for compressible blends in the weak segregation limit as a generalization of the standard random-phase approximation (RPA) formula for compressible systems. This weak segregation limit is indeed appropriate to the experimental data of Klein and co-workers.[14] Because the coexisting phases are at constant pressure, the homogeneous portion $\mathbf{F}_h$ of the functional $\mathbf{F}$ is written as

$$\mathbf{F}_h = \int_{-\infty}^{\infty}dz\,[-f(\phi_1,\phi_2) + \mu_1^*\phi_1 + \mu_2^*\phi_2 + Pv_{cell}/k_BT] \tag{2.19}$$

where $f(\phi_1,\phi_2) \equiv F/(N_lk_BT)$ is the specific Helmholtz free energy, P is the constant pressure in the bulk phases, and $\mu_\alpha^* \equiv \mu_\alpha/(M_\alpha k_BT)$ is the dimensionless chemical potential of polymer species α (in one of the coexisting phases) per occupied lattice site. The free energy F and chemical potential μ_α are provided by the LCT from eqs 2.1 and 2.9, respectively.

Minimizing the free energy functional in eq 2.17 with respect to the independent variations $\delta\phi_1(z)$ and $\delta\phi_2(z)$ leads to the set of two nonlinear second-order differential equations,

$$\frac{c_1}{\phi_1}\frac{d^2\phi_1}{dz^2} + \frac{c_1}{2\phi_1^2}\left(\frac{d\phi_1}{dz}\right)^2 + \frac{\partial f}{\partial\phi_1} - \mu_1^* = 0 \tag{2.20a}$$

$$\frac{c_2}{\phi_2}\frac{d^2\phi_2}{dz^2} + \frac{c_2}{2\phi_2^2}\left(\frac{d\phi_2}{dz}\right)^2 + \frac{\partial f}{\partial\phi_2} - \mu_2^* = 0 \tag{2.20b}$$

with the boundary conditions

$$\phi_1(z=\infty) = \phi_1^{(I)}, \quad \phi_1(z=-\infty) = \phi_1^{(II)} \tag{2.21a}$$

$$\phi_2(z=\infty) = \phi_2^{(I)}, \quad \phi_2(z=-\infty) = \phi_2^{(II)} \tag{2.21b}$$

in the coexisting homogeneous phases and with $c_\alpha \equiv l_\alpha^2/18$. The set of second-order nonlinear differential equations in eq 2.20 is numerically unstable. Therefore, special procedures have been developed[12] based on a combination of variational and perturbation methods to generate the solutions $\phi_1(z)$ and $\phi_2(z)$ which describe the composition variation $\Phi_1(z) = \phi_1(z)/[\phi_1(z) + \phi_2(z)]$ and the density fluctuation $\phi(z) = \phi_1(z) + \phi_2(z)$ through the interfacial profile. The theory for compressible binary blend interfaces has been presented[11] for symmetric blends, but a future paper[12] will provide the generalization of the interfacial theory to compressible blends with both molecular weight ($N_1 \neq N_2$) and interaction ($\epsilon_{11} \neq \epsilon_{22} \neq \epsilon_{12}$) asymmetries, as well as with different monomer molecular structures.

III. LCT Computations for PSD/PSH Blends

This section summarizes the LCT computations of the effective interaction parameter, coexistence curve, and interfacial profile for PSD/PSH blends as well as the direct comparison of calculated properties with experimental data.

The PSD/PSH blend is depicted in the generalized lattice model by a mixture of chains with N_α (α = 1 and 2) structured monomers whose structures are identical for both components. Each individual monomer extends over s = 9 lattice sites and has the structure displayed in Figure 1. Apart from having $N_1 \neq N_2$, the only difference between the two blend components in our model arises by ascribing different self-interaction energies $\epsilon_{\alpha\alpha}$ to the deuterated and hydrogenated polystyrene species and a

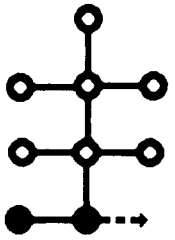

Figure 1. Lattice model of a styrene monomer. Circles denote monomer portions that occupy single lattice sites, and lines depict bonds which are fully flexible in three-dimensional space. Solid circles in the model designate monomer portions belonging to the backbone chain, and the arrow indicates the direction of linkages between consecutive monomers in the polymer chains.

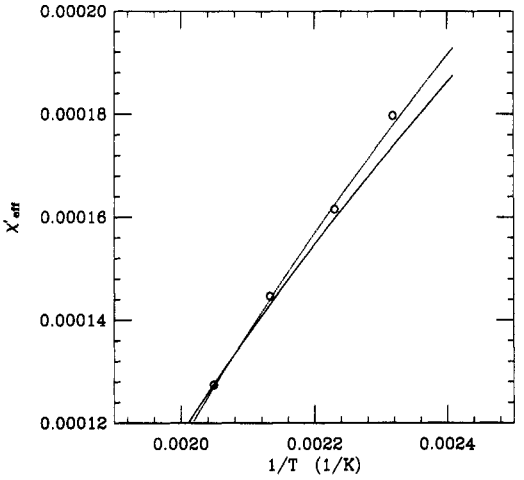

Figure 2. LCT computations of the effective interaction parameter χ'_{eff} as a function of the inverse temperature $1/T$ for the PSD/PSH blend with polymerization indices $N_{PSD} \equiv N_1 =$ 11 500 and $N_{PSH} \equiv N_2 = 8700$ at $P = 1$ atm and $\Phi_1 = 0.5$. The solid line is obtained for $\epsilon_{11}/k_BT_0 = 0.5$, $\epsilon_{22}/k_BT_0 = 0.5015$, and $\epsilon_{12}/k_BT_0 = 0.500\,742\,2$ ($T_0 = 415.15$ K), while the dotted line corresponds to the set of slightly different interaction energies, $\epsilon_{11}/k_BT_0 = 0.5$, $\epsilon_{22}/k_BT_0 = 0.501$, and $\epsilon_{12}/k_BT_0 = 0.500\,491\,6$. Circles denote the experimental data of Londono et al.[2]

different interaction energy ϵ_{DH} between the two components. The present theory employs the simplest model with the three independent van der Waals energies $\epsilon_{11} = \epsilon_{DD}$, $\epsilon_{22} = \epsilon_{HH}$, and $\epsilon_{12} = \epsilon_{DH}$, which are treated as adjustable parameters. However, since the self-interaction energy ϵ_{11} has already been determined from our previous fits[13] of the LCT predictions to experimental data for PSD/PVME blends, we fix this interaction energy as $\epsilon_{11} = 0.5k_BT_0$ ($T_0 = 415.15$ K), leaving only two adjustable parameters. The observation of an upper critical solution temperature phase diagram suggests the condition $\epsilon_{11} + \epsilon_{22} - 2\epsilon_{12} > 0$. Prior discussions[6] of isotopic blends argue that the $\epsilon_{\alpha\beta}$ should be proportional to the products of polarizabilities (or equivalently to monomer volumes) for the α and β species groups (occupying single lattice sites). If correct, this polarizability model requires that $\epsilon_{22}/\epsilon_{11} > 1$ and $\epsilon_{12} = (\epsilon_{11}\epsilon_{22})^{1/2}$. Our comparisons below with the experiment provide a first quantitative test of this polarizability model by allowing ϵ_{12} and ϵ_{22} to be adjustable parameters and by using the molecular-based LCT.

Calculations of the LCT effective interaction parameter χ_{eff} of eq 2.5 are performed assuming complete scattering contrast since the computed corrections from scattering by protonated monomers are found numerically to be negligible for the PSD/PSH systems. Figure 2 displays the temperature dependence of the monomer–monomer effective interaction parameter χ'_{eff} predicted by the LCT (solid line) along with experimental data of Londono et al.[2] (circles) for a PSD/PSH sample with $N_1 = N_{PSD} =$ 11 500, $N_2 = N_{PSH} = 8700$, and $\Phi_1 = 0.5$. The three $\epsilon_{\alpha\beta}$ are $\epsilon_{11} = 0.5k_BT_0$, $\epsilon_{22} = 0.501k_BT_0$, and $\epsilon_{12} = 0.5004916k_BT_0$. The fit is, however, not unique as there appears to be a continuous range of ϵ_{22} and ϵ_{12} that equally well reproduces the experimental data. Another set of the three $\epsilon_{\alpha\beta}$, for instance, is $\epsilon_{11}/k_BT_0 = 0.5$, $\epsilon_{22}/k_BT_0 = 0.5015$, and $\epsilon_{12}/k_BT_0 = 0.500\,742\,2$, and this set provides a fit of similar quality (dotted line in Figure 2). We anticipate that fits are also possible for ϵ_{22}/k_BT_0 in the range of 0.501 to 0.5015 (with suitably adjusted ϵ_{12}), but the quality of the fit degrades for $\epsilon_{22}/k_BT_0 > 0.5015$.

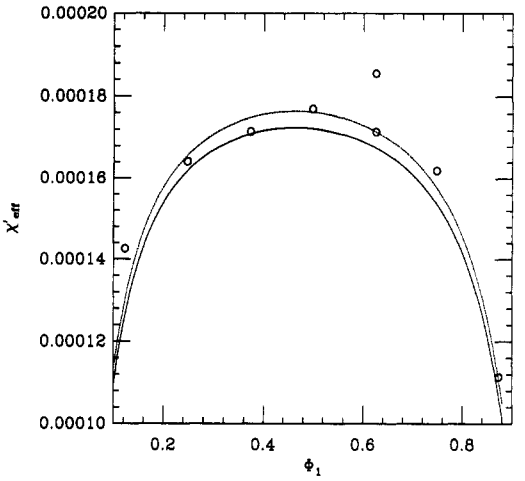

Figure 3. LCT computations of the effective interaction parameter χ'_{eff} as a function of composition $\Phi_{PSD} \equiv \Phi_1$ for the PSD/PSH blend with $N_1 = 11\,500$ and $N_2 = 8700$ at $P = 1$ atm and $T = 433.15$ K. The solid curve is obtained for $\epsilon_{11}/k_BT_0 = 0.5$, $\epsilon_{22}/k_BT_0 = 0.5015$, and $\epsilon_{12}/k_BT_0 = 0.500\,742\,2$ ($T_0 = 415.15$ K), while the dotted curve corresponds to the calculations with $\epsilon_{11}/k_BT_0 = 0.5$, $\epsilon_{22}/k_BT_0 = 0.501$, and $\epsilon_{12}/k_BT_0 = 0.500\,491\,6$. Circles denote experimental data of Londono et al.[2]

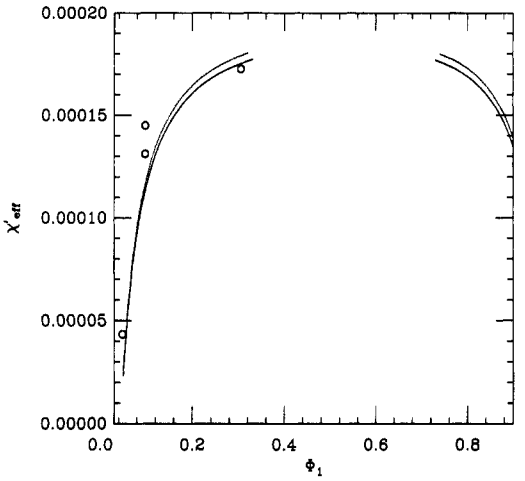

Figure 4. Same as Figure 3 but for the PSD/PSH sample with different polymerization indices, $N_1 = 11\,500$ and $N_2 = 15\,400$.

The computed composition dependence of the effective interaction parameter χ'_{eff} is in very good agreement with experiment[2] for both of the above parameter sets. Figure 3 depicts the computed χ'_{eff} versus composition Φ_1 at the constant temperature $T = 433.15$ K for the same PSD/PSH sample. The two concave downward curves in Figure 3 are obtained by using the two slightly different sets of $\{\epsilon_{\alpha\beta}\}$ described above. A concave downward shape of the $\chi'_{eff}(\Phi_1)$ curve is also found for another PSD/PSH sample (with $N_1 = 11\,500$ and $N_2 = 15\,400$) as depicted in Figure 4, where the LCT predictions again agree with the experimental data.[2] The gap in the theoretical curves χ'_{eff}

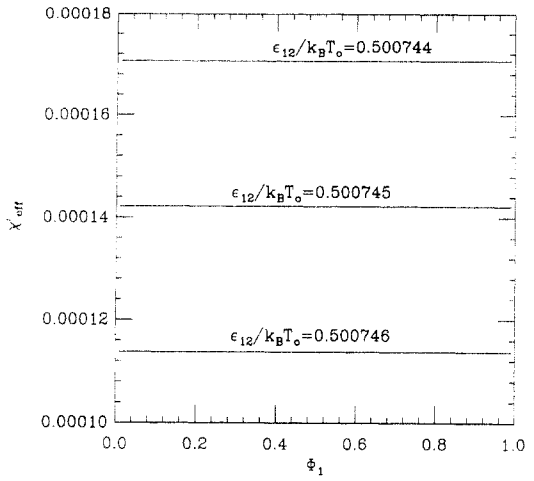

Figure 5. LCT computations of the effective interaction parameter χ'_{eff} as a function of composition Φ_1 for the hypothetical incompressible PSD/PSH blend with N_1 = 11 500 and N_2 = 8700 at T = 433.15 K. The self-interaction energy parameters are chosen as ϵ_{11}/k_BT_0 = 0.5 and ϵ_{22}/k_BT_0 = 0.5015 (T = 415.15 K), while the values of ϵ_{12} used in the calculations are indicated on the figure.

(Φ_1) of Figure 4 between $\Phi_1 \simeq 0.32$ and $\Phi_1 \simeq 0.73$ stems from the calculated phase separation which occurs within this composition range.

Additional LCT calculations have been performed for incompressible models of PSD/PSH blends to study the influence of equation of state effects on the composition dependence of $\chi_{eff}(\Phi_1)$. (The incompressible limit calculations follow trivially by setting $\phi_v = 0$ in the free energy of eq 2.1). While the ϵ_{11} and ϵ_{22} for the incompressible blend are taken as the same as those used in the computations for compressible blends, ϵ_{12} is varied slightly from ϵ_{12}/k_BT_0 = 0.500 742 2 to ensure the existence of a homogeneous one-phase incompressible system at T = 433.15 K. Examples of this hypothetical incompressible blend limit behavior of $\chi'_{eff}(\Phi_1)$ are presented in Figure 5 for $\epsilon_{11} = 0.5k_BT_0$, $\epsilon_{22} = 0.5015k_BT_0$, and three different choices of ϵ_{12}. Note that the incompressible $\chi'_{eff}(\Phi_1)$ are independent of composition. Thus, these calculations suggest that the observed composition dependence of χ_{eff} (see Figures 3 and 4) arises from compressibility (or equation of state) effects. The LCT computations described in Figures 3 and 4 refer to a pressure of P = 1 atm and a temperature of T = 433.15 K, and the use of the equation of state yields ϕ_v = 0.176. This value of ϕ_v is generally consistent with the recent experimental estimation[22] of the free volume distribution in a pure PS melt.

Schwahn et al.[3] have also performed neutron scattering experiments for PSD/PSH blends. Their data for the effective interaction parameter Γ, defined by eq 2.11, cover a wider range of both compositions and temperatures than the data of Londono et al. The Schwahn et al. data[3] also exhibit a range in which Γ is negative, departing from the positive χ'_{eff} of Londono et al.[2] First of all, we are unable to obtain a universal fit to the temperature dependence of Γ over a wide composition range. Taking ϵ_{11} and ϵ_{22} as identical to those used in the LCT fit of Figure 2, a separate adjustment of ϵ_{12} is required to reproduce the data for each of the five compositions between Φ_1 = 0.093 and Φ_1 = 0.58. A reasonably good fit is obtained for $\epsilon_{11} = 0.5k_BT_0$, $\epsilon_{22} = 0.501k_BT_0$, and ϵ_{12}/k_BT_0 in the range of 0.50049985–0.5004918 as described in Figure 6a. This range involves a variation of the "physical" interaction energy ϵ_{12} in the sixth decimal place, corresponding to minuscule energy variations on the order of 10^{-3} cal/mol of styrene segments. However, this tiny variation induces a much larger

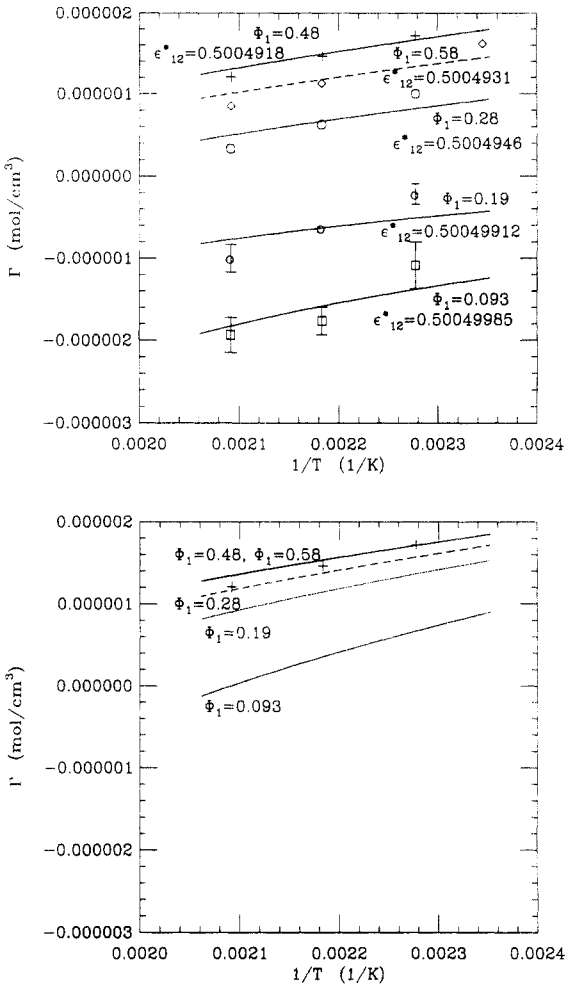

Figure 6. (a) LCT computations of the effective interaction parameter Γ as a function of the inverse temperature $1/T$ for the PSD/PSH sample with N_1 = 8750 and N_2 = 9904 at P = 1 atm. The self-interaction energies are chosen as ϵ_{11}/k_BT_0 = 0.5 and ϵ_{22}/k_BT_0 = 0.501, while the separately adjusted values of the $\epsilon^*_{12} \equiv \epsilon_{12}/k_BT_0$ (T = 415.15 K) for each Φ_1 are specified on the figure. Experimental data are taken from the work of Schwahn et al.[3] (b) Same as a but for interaction energies identical to those used in Figure 2. Crosses denote the experimental data of Schwahn et al.[3] for Φ_1 = 0.48.

percentage spread in the exchange energy $\epsilon/k_BT_0 \equiv (\epsilon_{11} + \epsilon_{22} - 2\epsilon_{12})/k_BT_0$ which varies between 3.0×10^{-7} (for Φ_1 = 0.093) and 1.64×10^{-5} (for Φ_1 = 0.48). Figure 6b is drawn with the same scale as Figure 6a and displays the LCT predictions of the temperature dependences $\Gamma(\Phi_1 = const, 1/T)$ generated for the same $\{\epsilon_{\alpha\beta}\}$ as used in reproducing data of Londono et al.[2] The fit is only satisfactory for the intermediate compositions in the range of Φ_1 = 0.48. The Londono et al.[2] data for $\chi'_{eff}(1/T)$ correspond to a composition of Φ_1 = 0.5, which is close to the value Φ_1 = 0.48 where the same parameters also fit the Schwahn et al.[3] temperature dependence. Furthermore, our ability to reproduce the Schwahn et al. data with a very small range for the physical interaction ϵ_{12} indicates that the LCT admits the presence of negative χ'_{eff} or Γ in "repulsive" systems with positive exchange energy ϵ. As previously noted[5] by us, this possible appearance of a negative effective interaction parameter is a direct consequence of equation of state effects and emphasizes the inadequacy of interpreting χ'_{eff} from eq 2.10 or Γ from eq 2.11 with a microscopic interaction energy ϵ. Note that the substantial entropic contribution to the experimental χ_{eff} in Figures 2 and 6 similarly suggests the inadequacy of models based only on interaction asymmetries.

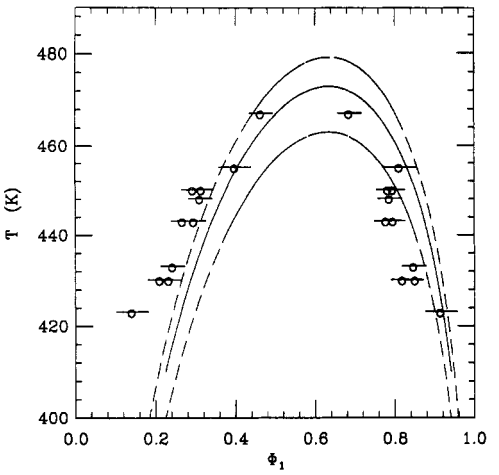

Figure 7. LCT computations of the coexistence curve for the PSD/PSH sample with $N_1 = 9196$ and $N_2 = 27\,788$ at $P = 10^{-5}$ Torr. The three curves are obtained for the same self-interaction energies ($\epsilon_{11}/k_BT_0 = 0.5$ and $\epsilon_{22}/k_BT_0 = 0.501$), but slightly different $\epsilon_{12}/k_BT_0 = 0.500\,492\,5$, 0.500 492 7 and 0.500 493 0 (top to bottom). Circles denote experimental data of Budkowski et al.[14]

Examples of the LCT predictions for the coexistence curve (at $P = 10^{-5}$ Torr) are computed from eqs 2.16 and are presented in Figure 7 along with experimental data of Budkowski et al.[14] The three curves of Figure 7 are obtained for the same $\epsilon_{11}/k_BT_0 = 0.5$ and $\epsilon_{22}/k_BT_0 = 0.501$, but for the three very slightly different interactions $\epsilon_{12}/k_BT_0 = 0.500\,492\,5$, 0.500 492 7, and 0.500 493 0, which would be experimentally indistinguishable as interaction energies. A small change in the interaction energy ϵ_{12} by $3 \times 10^{-7} k_BT_0 = 2 \times 10^{-3}$ cal/mol of styrene monomers, however, shifts the computed critical temperature by about 10 K, again stressing the futility at computing such interactions from first principles or from empirical potential functions. The three calculated coexistence curves in Figure 7 have a spread that far exceeds the experimental errors, but they display good agreement with the experimental data[14] which are obtained from direct measurements using nuclear reaction analysis. The three ϵ_{12} (and also the three corresponding ϵ) employed in the above LCT computations of the coexistence curve are very close to those used in the fit to the SANS data of Londono et al., indicating very good internal consistency between these two sets of data.

Reasonably good agreement with experimental data[14] is likewise found for the interfacial profile computed from eqs 2.20 and 2.21 and from the LCT free energy (eq 2.1). Figure 8a illustrates the composition profile $\Phi_{PSD}(z)$ through the planar interface in a phase-separated PSD/PSH blend at $T = 443.15$ K and $P = 10^{-5}$ Torr. The three theoretical curves of Figure 8a are generated for the same three sets of $\{\epsilon_{\alpha\beta}\}$ as for the coexistence curves in Figure 7 using a compressible blend theory and the weak segregation limit which is reasonably appropriate to the experimental system with radii of gyration of 80 and 134 nm, respectively, for PSD and PSH. The calculated compositions in the bulk coexisting phases at $T = 443.15$ K depart somewhat from experimental data (see Figure 7), leading to some shifts between the theoretical and experimental[14] interfacial profiles. However, the effective profile width $w = (\Phi_1^{(I)} - \Phi_1^{(II)})/[d\Phi_1/dz]_{center}$, which provides one overall measure of the profile shape, is close to the experimental value of $w \simeq 145$ nm. The three choices for the energetic parameters yield widths ranging from $w = 138$ nm to $w = 194$ nm. Figure 8b provides an additional illustration of the consistency between the calculated and experimetnal shapes of the interfacial

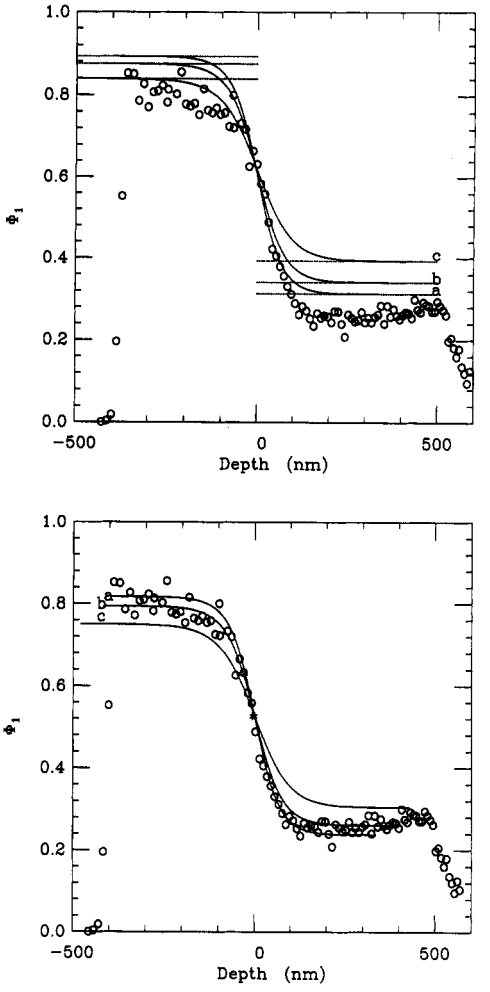

Figure 8. (a) LCT computations of the composition profile $\Phi_1(z)$ through the planar interface in the phase-separated PSD/PSH blend with $N_1 = 9196$ and $N_2 = 27\,788$ at $T = 443.15$ K and $P = 10^{-5}$ Torr. The three profiles are obtained for the same $\epsilon_{11}/k_BT_0 = 0.5$ and $\epsilon_{22}/k_BT_0 = 0.501$ ($T_0 = 415.15$ K) but slightly different $\epsilon_{12}/k_BT_0 = 0.500\,493\,0$ (curve a), $\epsilon_{12}/k_BT_0 = 0.500\,492\,7$ (curve b), and $\epsilon_{12}/k_BT_0 = 0.500\,492\,5$ (curve c). The dotted horizontal lines indicate the compositions in the bulk coexisting phases and are drawn as a guide for the eye. The Kuhn lengths l_1 and l_2 are assumed as identical, $l_1 = l_2 = 6.8$ Å. Experimental data (circles) are taken from the work of Budkowski et al.[14] (b) Superimposed LCT profiles from (a) that are obtained by shifting their centers to the center of the experimental profile of Budkowski et al.[14] This common center is placed at $z = 0$.

profiles. The theoretical profiles of Figure 8a are shifted in Figure 8b to make their centers coincide with the center of the experimental profile of Budkowski et al.[14]

All computations described in this section are carried out for $v_{cell} = [(v_1v_2)/(s_1s_2)]^{1/2} = 18.550\,346$ Å^3, where the volumes v_1 and v_2 of perdeuterated and hydrogenated styrene monomers are assumed to be identical and equal to $v_1 = v_2 \simeq 166.953$ Å^3. The later value corresponds to the molar volume V_{PSD} of deuterated styrene $V_1 \equiv V_{PSD} = 100.54$ cm^3/mol that has been employed in our previous fits[13] to the experimental data for PSD/PVME blends. However, the computed properties at $P = 1$ atm and $P = 10^{-5}$ Torr in Figures 2–8 are found to be numerically unchanged by using values of v_{cell} estimated from the v_1 and v_2 given by different sources (for instance, by refs 2 and 3).

IV. SANS Data and Computations for Other Isotopic Blends

Considerable controversy and confusion exist in the literature concerning the composition dependence of the

experimental small-angle neutron scattering (SANS) effective interaction parameter χ_{eff} for isotopic blends. The SANS experiments of Bates et al.[4] display a strong parabolic upward dependence of χ'_{eff} on composition in poly(vinylethylene) (PVE) and poly(ethylethylene) (PEE) isotopic blends. A similar behavior of χ'_{eff} with composition has been recently reported[2] also for polyethylene (PE) isotopic mixtures. On the other hand, both Schwahn et al.[3] and Londono et al.[2] observe a much weaker and parabolic downward composition dependence of the effective interaction parameter for polystyrene (PSD/PSH) isotopic blends. As demonstrated in section III, the observations for PSD/PSH blends are successfully described by the compressible lattice cluster theory (LCT).

The polarizability model suggests that the ratios of $\epsilon_{\alpha\beta}$'s for isotopic blends lie within 1–2% of unity. If the ratios differ by more than a few percent from unity, the model systems are called "strongly interacting" and are inappropriate for describing isotopic blends. Compressible blend LCT computations with a range of interaction energies *appropriate to isotopic blends* fail to predict a substantial parabolic upward behavior of $\chi_{eff}(\Phi_1)$ for these systems in apparent contradiction with experimental measurements. In contrast, several other computations[17-20] in the literature are quoted as providing theoretical confirmation of the upward behavior, but as shown below all such computations contain one or more of the following deficiencies which make them either inappropriate for describing isotopic blends or unsuitable for representing the experimental conditions: Many theoretical studies use interaction parameters appropriate to strongly interacting systems, consider only very short chains, treat constant volume systems, or involve calculations for blends with unrealistically low densities or high pressures. Furthermore, the computations for the most reasonable models, if any, produce minuscule upward curvature of $\chi_{eff}(\Phi_1)$ (also possible from the LCT) compared to experimental observations. We, however, find no inconsistency in the different behaviors displayed by the χ_{eff} for isotopic blends because, as noted by Han and co-workers,[23] PVE and PEE are based on butadiene syntheses which yield random copolymers, while PE is branched[24] and therefore contains certain random copolymer character. We now explain why this copolymer randomness could swamp the subtle differences between H and D monomers. This speculative explanation is then followed by an analysis of the limitations of the often cited theoretical computations[17-20] for isotopic blends.

A. Influence of Randomness. First of all, PVE and PEE are obtained by hydrogenation (or deuteration) of 1,2- and 1,4-butadiene, respectively. It is, however, well-known that PVE or PEE are random copolymers with varying degrees of both 1,2- and 1,4-polybutadiene units and even some *cis* geometrical isomers. PVE has a majority of 1,2-butadiene monomers, while PEE has a majority of 1,4-butadiene segments. Thus, isotopic blends of PVE or of PEE are blends of random copolymers. Han and coworkers[23] have successfully modeled the χ_{eff} of polybutadiene blends using random copolymer theory, and they have even made the striking observation of both UCST and LCST phase behavior depending on the microstructure of the polybutadiene chains. It stands to reason that, if microstructure (i.e., random copolymer character) exerts such drastic influence on phase behavior, microstructure could overwhelm the effects of minute differences between H- and D-containing monomers.

Simple Flory–Huggins type descriptions of random copolymers indicate the existence of differences between χ_{eff} for a blend of homopolymers A and B′ and the χ_{eff} for a blend of random copolymers A_xB_y and $A'_{x'}B'_{y'}$, where the primes indicate deuterated species. We have already used[25] the molecularly based LCT to demonstrate different behaviors between χ_{eff} for homopolymer blends and the corresponding diblock copolymer melts as a function of composition, temperature, pressure, etc. Since the LCT has not yet been developed for random copolymer systems, our analysis is based upon the available theory[26] for diblock copolymer melts as follows: The LCT free energy coefficients f_{kl} in eq 2.1 are derived for diblock copolymers in the form,

$$f_{kl} = a_{kl} + b_{kl}/N + j_{kl}/N \tag{4.1}$$

where N is the polymerization index and the correction term b_{kl}/N emerges as a chain end correction, whereas the additional contribution of j_{kl}/N arises from the presence of the junction between the two blocks. The junction represents a more serious perturbation to the chain with $|j_{kl}| \gg |b_{kl}|$. The particular form of eq 4.1 should be anticipated because the LCT noncombinatorial free energy and its composition expansion coefficients f_{kl} are macroscopic quantites in contrast to the purely microscopic interaction parameter $\chi^{FH} = z(\epsilon_{11} + \epsilon_{22} - 2\epsilon_{12})/(2k_BT)$ of Flory–Huggins theory. We now use the form in eq 4.1 for a single junction to infer the behavior of the free energy for a mixture of random copolymers with many such junctions.

Let the number of junctions in a single random copolymer chain be cN with $c < 1$. This yields a junction correction to f_{kl} of roughly the order $(j_{kl}/N)cN = j_{kl}c$. Even when c represents a small fraction, the product $j_{kl}c$ can be comparable with the a_{kl} term from eq 4.1 and may have a significant impact on the observed χ_{eff} which depends on all the f_{kl} in a rather complicated fashion. Therefore, the parabolic upward dependence of χ'_{eff} on composition, which is observed in PVE and PEE isotopic blends by Bates et al.,[4] may be driven by the presence of random microstructure. Similar arguments pertain to the SANS data of Krishnamoorti et al.[27] for various isotopic blends derived from poly(ethylbutadiene) and polybutadienes. The importance of these microstructure effects has already been emphasized by many authors. Sakurai et al.[23] demonstrate that the miscibility of isotopic binary blends of polydienes cannot be explained solely on the basis of isotopic effects. Moreover, Jinnai et al.[28] provide experimental evidence for an inversion of the phase diagram from an UCST to LCST form with an increase of the vinyl content of the protonated PB in isotopic PB blends. This drastic change may only be predicted[28] using random copolymer theory.

High-density polyethylene, which is used in the SANS experiments of Londono et al.,[2] contains about 5% of CH_3, $-CH{=}CH_2$, $-CH{=}CH-$, and $=C{=}CH_2$ groups, and therefore also is a random copolymer. Even such a small percentage of these groups can grossly alter χ_{eff} and its composition dependence.

It may be argued that the inability of the LCT to obtain significant parabolic upward $\chi_{eff}(\Phi_1)$ arises because our extended model of isotopic blends does not consider different sizes between CD_2 and CH_2 monomers. Thus, we have performed LCT calculations of χ_{eff} for PE with an added size asymmetry entropic contribution χ_s that is taken from the PRISM theory of Curro and Schweizer,[8] who use a thread model to derive

$$\chi_s = -\frac{\eta^2\gamma^{-1/2}}{6}(\gamma - 1)^2[\Phi_1 + (1 - \Phi_1)/\gamma] \tag{4.2}$$

where η is the packing fraction, $\gamma \equiv \sigma_2/\sigma_1$ is the relative segment length ratio, and the subscript 1 refers to the deuterated species. Equation 4.2 represents the case where the statistical segment lengths σ_α and hard-core diameters d_α (α = 1 and 2) are equal to each other, and both chain lengths are large (N_1 and $N_2 \to \infty$). The packing fraction η is related to the free-volume fraction ϕ_v in the lattice model by

$$\eta = \eta_{rcp}(1 - \phi_v) \tag{4.2a}$$

with η_{rcp} = 0.70717 the random close packing fraction for a hard-sphere system. The appendix provides details of how the entropic contributions from the size asymmetry PRISM model of eq 4.2 are appended into the LCT computations. Using choices of $\{\epsilon_{\alpha\beta}\}$ suitable for isotopic blends, our LCT-size asymmetry model computations for PE isotopic mixtures (treated as binary homopolymer blends) never yield the parabolic upward composition behavior of χ_{eff} that is observed by Londono et al.[2] Although our generalized lattice model, with the added size asymmetry model entropic contribution χ_s to χ_{eff}, still represents an oversimplification of reality, we believe that the main failure of these calculations (and the ones for PVE and PEE isotopic blends) in reproducing experimental data[2,4] arises because PE should be treated as a randomly (lightly) branched chain (and because PVE and PEE are random copolymers). More conclusive arguments on this matter will be possible after generalizing the LCT to random copolymer systems. This highly nontrivial generalization is currently in progress.[29]

B. Other Theoretical Computations. Several theoretical computations are widely quoted in the literature by SANS experimentalists to illustrate "qualitative agreement" with experimental data for isotopic blends. However, these computations often apply to systems departing considerably from those appropriate to isotopic blends or from experimental conditions. Both PRISM computations of Schweizer and co-workers[17] and Monte Carlo simulations of Sariban and Binder[18,19] are performed for constant volume binary blends. Kumar[20] has demonstrated that χ_{eff} computed for constant volume and constant pressure systems often differ significantly. Kumar's simulations apply to strongly interacting blends, and we find less disparity between constant pressure and constant volume cases for our model parameters for isotopic PSD/PSH blends. The PRISM theory calculations employ the symmetric interaction blend model ($\epsilon_{11} = \epsilon_{22} = 0$, $\epsilon_{12} = -\epsilon$) which is also not appropriate to studying real isotopic blends because the vanishing of ϵ_{11} and ϵ_{22} implies that normal liquid densities appear only at astronomical pressures. A moderate upward parabolic variation of χ_{eff} with composition (see Figure 9a in ref 17) is predicted by PRISM theory only for very dilute systems with η = 0.2, corresponding to a dense "gas" with $\phi_v \simeq 0.7$. At normal liquid densities ($\eta \simeq 0.5$), the PRISM-computed composition dependence of χ_{eff} becomes minuscule[17] compared to the experimental data for isotopic blends. Moreover, the vanishing self-interaction energies ϵ_{11} and ϵ_{22} in the PRISM calculations favor the presence of free volume and inevitably produce high pressures in such a liquid system.

The interaction models used in the Monte Carlo simulations of Sariban and Binder[18,19] likewise do not represent real isotopic blends. A moderate parabolic upward behavior of χ_{eff} with composition (see Figures 8 and 15 of refs 19 and 18, respectively) is obtained only along the coexistence curve where the temperature changes significantly. At constant (higher) temperatures in the one-phase blend, the composition variation of χ_{eff} computed by Sariban and Binder is considerably smaller than that in the isotopic blend experiments. The Monte Carlo simulations of Kumar[20] for binary blends at constant pressure use models which are again not appropriate for isotopic blends as noted by him. For instance, the choice of $\epsilon_{12}/\epsilon_{11}$ = 1.2 and $\epsilon_{11} = \epsilon_{22}$, where $\epsilon_{\alpha\beta}$ is the monomer–monomer Lennard-Jones parameter between species α and β, departs from the very nearly identical interactions present in the isotopic systems. The downward parabolic composition dependence of χ_{eff} (bottom curve in Figure 9 of ref 20) computed by Kumar agrees qualitatively with that observed experimentally and predicted by the LCT for PSD/PSH isotopic blends, but Kumar's interaction parameters apply to a system with highly asymmetric interactions. By choosing $\epsilon_{12}/\epsilon_{11}$ = 0.9, Kumar[20] is also able to generate a convex parabolic curve $\chi_{eff}(\Phi_1)$. This finding is consistent with our previous LCT computations[16] for binary blends with low molecular weights and stronger (i.e., more asymmetric) relative interactions than in isotopic blends.

Both of the above-described simulations[18-20] are performed for very short polymer chains, and we have shown[16] the strong, even qualitative, difference in the composition dependence of χ_{eff} which emerges upon variation of polymerizarion indices from small to large N_α, especially when the interaction energies $\epsilon_{\alpha\beta}$ are fairly unsymmetrical. In conclusion, existing theoretical computations do not support the occurrence for nonrandom isotopic blends of a parabolic upward $\chi_{eff}(\Phi_1)$ with magnitudes comparable to those presented by experiments for random copolymer isotopic blends.

V. Discussion

Available small-angle neutron scattering experiments for isotopic blends raise important questions concerning the composition dependence of the effective interaction parameter χ'_{eff}. Experiments find that χ'_{eff} is a concave function of composition for PSD/PSH blends, while it displays a convex behavior for PVE, PEE, and PE isotopic mixtures. This difference in composition dependences presents a real challenge to theories of polymer fluids, especially those suggesting that a universal mechanism, based on differences in molecular volumes and polarizabilities of the two components, governs the behavior of χ'_{eff} for isotopic blends.

We study the PSD/PSH isotopic blend with the lattice cluster theory (LCT). The LCT combines a treatment of local correlations, monomer molecular structure, and blend compressibility, as well as of asymmetries in interactions, molecular weights, and monomer structures, features which distinguish the LCT from other theories that are unable to reproduce quantitatively experimental data for these isotopic blends. All the above features contribute to the predicted composition dependence of χ_{eff} in asymmetric systems and may likewise be expected to be important in describing isotopic mixtures where only subtle differences exist between hydrogenated and perdeuterated chains of the same chemical species. Since the generalized lattice model prescribes the same monomer structure to both components of an isotopic blend, the LCT is incapable of directly modeling size asymmetry of these systems, in spite of the fact that the generalized lattice model is specially designed to represent this feature of real blends. One possible remedy for such deficiency of the generalized lattice model involves absorbing all influences of size asymmetry into asymmetrical interaction energies, while another involves appending into the LCT computations of χ_{eff} the entropic size asymmetry contribution χ_s from

the PRISM continuum thread model of Curro and Schweizer.[8] Our calculations for PE isotopic blends indicate, however, that the latter modification does not qualitatively alter the computed composition dependence of χ_{eff}.

As demonstrated in section III, the LCT successfully describes the experimental observations for PSD/PSH blends. Our computations for PSD/PSH blends yield the very slightly asymmetric interaction energy parameters $\epsilon_{22}/\epsilon_{11} = 1.002$ and $\epsilon_{12}/\epsilon_{11} \simeq 1.001$. Computations for a similar incompressible blend suggest that the observed concave behavior of $\chi'_{eff}(\Phi_1)$ stems from substantial equation of state effects, while the significant calculated and observed entropic contributions to $\chi_{eff}(\Phi_1)$ indicate that its behavior is governed by more than just interaction asymmetries. The above-quoted ratios of the $\epsilon_{\alpha\beta}$'s from the LCT fits to SANS data depart quite considerably from those implied by the polarizability (or monomer volume) model,

$$\frac{\epsilon'_{22}}{\epsilon'_{11}} \simeq \frac{\alpha_H^2}{\alpha_D^2} \simeq 1.029 \tag{5.1}$$

and

$$\frac{\epsilon'_{12}}{\epsilon'_{11}} \simeq \frac{\alpha_H}{\alpha_D} \simeq 1.015 \tag{5.2}$$

where α_H and α_D designate respectively the polarizabilities of protonated and perdeuterated styrene monomers, and the numerical estimates in eqs 5.1 and 5.2 are taken from data in ref 6 for toluene. Equations 5.1 and 5.2 thereby further illustrate the inadequacy of the polarizability model for the estimation of the van der Waals attractive energies $\epsilon_{\alpha\beta}$. The polarizability model emerges from a consideration of long-range van der Waals interactions, on the one hand, and zero point vibration contributions to the monomer volume, on the other. However, most of the styrene molecule's polarizability arises from the conjugated π-electron system. Consequently, the ratios of polarizabilities of the H and D styrene monomers are not good measures of their relative sizes. As is well-known, the structure of dense fluids is dominated by the repulsive forces. Isotope effects on the repulsive interactions arise, as noted above, from differences in H and D zero point vibrations, which yield differing sizes and, hence, densities, etc., for PSD and PSH of identical polymerization indices. These zero point vibration-induced size differences are, however, only incremental to the already large size of the benzene ring. Thus, there is no reason to expect the $\epsilon_{\alpha\beta}$ for styrene to scale as the product of monomer polarizabilities.

Good agreement is also found between experimental data and the LCT predictions for other properties, such as the coexistence curve and the interfacial profile in phase-separated PSD/PSH blends (see Figures 7 and 8). The latter properties are likewise described with a compressible theory, and this treatment of several different properties yields additional confirmation for the LCT description of the SANS data in Figures 2–6. Klein and co-workers[14] provide an alternative fit to their experimental coexistence curve for a PSD/PSH blend by using FH theory and by endowing χ'_{eff} with a weak linear composition dependence, but Budkowski has informed us that they have also made fits (unpublished) with the quadratic form of χ. The quality of their fit is better than that obtained from the LCT, and a postulated quadratic dependence of χ'_{eff} would agree better with the behavior observed in SANS experiments.[2,3] In addition, the LCT computations in Figure 5 show that χ'_{eff} becomes composition independent for the (infinite pressure) incompressible PSD/PSH blend limit. Hence, a simultaneous fit to both types of measurements is possible only when PSD/PSH blends are treated as compressible systems.

The interaction energy ϵ_{12} is adjusted for given ϵ_{11} and ϵ_{22} to reproduce experimental data for three different properties (effective interaction parameter, coexistence curve, and interaction profile). However, the fitted ϵ_{12} for different data vary in the sixth decimal place, a variation which is on the order of 10^{-3} cal/mol of styrene monomers and which is experimentally indistinguishable. On the other hand, a measurable difference is generated in the exchange energy $\epsilon = \epsilon_{11} + \epsilon_{22} - 2\epsilon_{12}$. The LCT and the extended lattice model still represent an oversimplification of reality. Several improvements to the model and theory are possible, such as the use of different interaction parameters for aliphatic and aromatic groups, local stiffness, etc. These extensions lead to the presence of additional adjustable parameters and should improve agreement with experiment. However, we prefer to avoid the use of additional parameters unless warranted by the presence of gross discrepancies from experimental data.

The binary blend LCT fails to reproduce the experimental data for $\chi'_{eff}(\Phi_1)$ of isotopic PVE, PEE, and PE blends. This negative result is not a surprise since isotopic blends of PVE or of PEE are mixtures of random copolymers, while PE is branched and, therefore, displays certain random copolymer characteristics. As explained in section IV, copolymer randomness may readily swamp the isotopic effect arising from tiny size and interaction differences between H- and D-containing monomers. The recent observation[28] of an inversion of the phase diagram from UCST to LCST form with an increase in the vinyl content of the protonated PB in isotopic PB blends best illustrates the crucial importance of microstructure. If microstructure changes can drastically change the phase behavior, the same microstructure can easily alter the composition dependence of χ'_{eff} as well. Additional support for the strong influence of microstructure on χ'_{eff} emanates from theoretical considerations based on the LCT predictions for diblock copolymers with single junctions and a simple qualitative extension of this theory to random copolymers with many such junctions. Likewise, a small percentage of branched groups in PE is expected to introduce behavior much like a random copolymer and thereby to exert a significant impact on χ'_{eff}. Therefore, computations for isotopic PVE, PEE, and PE blends should be based on a theory of random copolymer systems in order to extract meaningful microscopic information about these blends from available experimental data. However, until such a molecular-based random copolymer theory is developed, our explanation based on randomness may only be considered as a speculation which suggests promising avenues for further exploration.

Several existing theoretical computations and Monte Carlo simulations are often quoted in the literature as a confirmation of the parabolic upward behavior of χ'_{eff}. However, these computations all contain some of the following ingredients, making them inappropriate for describing isotopic blends: (1) Some computations consider systems with far too large interaction asymmetries for representing isotopic blends. (2) Computations for constant volume systems may not be suitable for interpreting experiments at constant pressure. (3) Some model computations are performed for blends which have unrealistically high pressures or low densities. (4) Many

computations apply to rather short chains which may display a qualitatively different composition dependence for χ_{eff} than the longer chains considered experimentally. We find no fault with the quoted computations per say, only with their applications to the isotopic blend data. It remains to be seen, however, whether random copolymer type theories can explain not only the SANS data for PVE, PEE, and PE isotopic blends but also other thermodynamic data for these systems.

Considerable effort is being devoted to developing a microscopic molecule-based understanding for the properties of polymer blends. Thus, new experimental and theoretical techniques have been generated for probing molecular consequences of blend properties. The dramatic phenomena exhibited by isotopic polymer blends have singled these systems out for special study in attempts at relating microscopic structures and interactions to observed blend properties. Our lattice cluster theory computations for PSD/PSH blends and qualitative arguments for certain other isotopic blends again focus upon several stringent requirements for extracting meaningful microscopic information for polymer blends. First, the theory must have sufficient microscopic realism to warrant the comparisons with experiments. One essential ingredient is the treatment of blends as compressible systems which therefore exhibit nontrivial equation of state effects. Other important features involve descriptions of size and shape asymmetries and perhaps specific interactions in some cases. The enormous complexity of polymer systems implies that microscopic theories must be deficient in certain respects, and the introduction discusses several limitations of the lattice cluster theory. Thus, in order to consider comparisons with experimental data, the theory needs to rely on some empiricism as the relevant energy differences in polymer blends are far too small for direct or even molecular mechanics computations. The theoretical goal[13,30] lies, therefore, in providing a comprehensive description for a variety of blend properties. For this purpose, experiments are expected to contribute data for a wide range of properties to overdetermine the theoretical parameters and to provide guidance for the further improvement in theories based, of necessity, on oversimplified models.

The PSD/PSH system has been chosen for LCT computations because of the availability of the maximum amount of data (and the absence of random copolymer complications) concerning the composition, temperature, and molecular weight dependence of the extrapolated small-angle neutron scattering (SANS), the coexistence curve, and the interfacial profile for the phase-separated blends. Even this wealth of data is insufficient in uniquely fixing the two available parameters of the compressible LCT, but the data do prescribe narrow ranges for the parameters. The LCT computations provide an excellent reproduction for the composition and temperature dependence of SANS data of Londono et al.,[2] with a less satisfactory treatment of the composition dependence for the data of Schwahn et al.[3] The computed coexistence curve is in reasonable agreement with experiments by Klein and co-workers,[14] while the composition profile is brought into quite good accord with experiment by shifting the profile to adjust for deficiencies in the computed coexistence curve. A fully compressible theory is used for computing the interfacial profiles, and the rather nontrivial extension of this theory to asymmetric systems will be given elsewhere.

Acknowledgment. This research is supported, in part, by NSF DMR Grant No. 92-23804 and has benefitted from the use of MRL (NSF) facilities at the University of Chicago. We thank Frank Bates for sending us a preprint of his paper and Jacob Klein and Andrzej Budkowski for providing us the original data for the coexistence curve and the interfacial profile for phase-separated PSD/PSH blends.

Appendix: Size Asymmetry Model

The entropic contribution χ_s is derived from the PRISM theory[31] in the form of eq 4.2 for a threadlike chain model where the two blend components have different monomer sizes. The presence of this size asymmetry affects the total scattering $S(0)$ and, hence, the total effective interaction parameter χ_{eff} which is defined in terms of $S(0)$. Since the generalized lattice model cannot describe the H/D monomer size asymmetry, we append the PRISM contribution χ_s to the LCT by utilizing the correspondence[32] between the PRISM theory[31] and the compressible random-phase approximation[32] (CRPA). The CRPA is equivalent to the PRISM theory[31] when the long wavelength limit of the Fourier transform $\hat{C}_{\alpha\beta}(k)$ of the direct correlation function $C_{\alpha\beta}$ and the LCT macroscopic interaction parameter $\chi_{\alpha\beta}$ between the α-β monomer pairs are related to each other by

$$\hat{C}_{\alpha\beta}(k=0) = 2\chi_{\alpha\beta} - (1/\phi_v) \tag{A.1}$$

First, we decompose the χ_s from eq 4.2 into the three separate contributions χ_{11}^{PRISM}, χ_{22}^{PRISM}, and χ_{12}^{PRISM} as

$$\chi_{\alpha\beta}^{PRISM} = \chi_s\gamma^{-(\alpha+\beta-2)}/(\gamma^{-1}-1)^2 \tag{A.2}$$

which satisfy the relation

$$\chi_{11}^{PRISM} + \chi_{22}^{PRISM} - 2\chi_{12}^{PRISM} = \chi_s \tag{A.3}$$

Then the PRISM corrections are added to the corresponding LCT macroscopic interaction parameters $\chi_{\alpha\beta}^{LCT}$,

$$\chi_{\alpha\beta} = \chi_{\alpha\beta}^{LCT} + \chi_{\alpha\beta}^{PRISM} \tag{A.4}$$

Reference 33 describes the method of calculating the $\chi_{\alpha\beta}^{LCT}$ from the LCT free energy in eq 2.1. The next step in the present model calculations involves determining a new $S_{11}(0)$ (or a set of $\{S_{\alpha\beta}(0)\}$ if the scattering contrast is incomplete) from the CRPA theory with the $\chi_{\alpha\beta}$ of eq A.4. The new effective interaction parameter χ_{eff} then follows from the analog of eq 2.5. We refer the interested reader again to ref 33 for more details.

References and Notes

(1) de Gennes, P.-G. *Scaling Concepts in Polymer Physics*; Cornell University Press: Ithaca, NY, 1979.
(2) Londono, J. D.; Narten, A. H.; Wignal, G. D.; Honnell, K. G.; Hsieh, E. T.; Johnson, T. W.; Bates, F. S. *Macromolecules* **1994**, *27*, 2864.
(3) Schwahn, D.; Hahn, K.; Streib, J.; Springer, T. *J. Chem. Phys.* **1990**, *93*, 8283.
(4) Bates, F. S.; Muthukumar, M.; Wignall, G. D.; Fetters, L. J. *J. Chem. Phys.* **1988**, *89*, 535.
(5) Dudowicz, J.; Freed, K. F. *Macromolecules* **1990**, *23*, 1519.
(6) Bates, F. S.; Fetters, L. J.; Wignall, G. D. *Macromolecules* **1988**, *21*, 1086.
(7) Bawendi, M. G.; Freed, K. F. *J. Chem. Phys.* **1988**, *88*, 2741.
(8) Curro, J. G.; Schweizer, K. S. *Macromolecules* **1990**, *23*, 1402.
(9) Freed, K. F.; Bawendi, M. G. *J. Phys. Chem.* **1989**, *93*, 2194. Dudowicz, J.; Freed, K. F.; Madden, W. G. *Macromolecules* **1990**, *23*, 4803.
(10) Dudowicz, J.; Freed, K. F. *Macromolecules* **1991**, *24*, 5074.
(11) Lifschitz, M.; Freed, K. F. *J. Chem. Phys.* **1993**, *98*, 8994.
(12) Lifschitz, M.; Freed, K. F., manuscript in preparation.
(13) Dudowicz, J.; Freed, K. F. *Macromolecules* **1991**, *24*, 5112.

(14) Budkowski, A.; Steiner, U.; Klein, J. *J. Chem. Phys.* **1992**, *97*, 5229. Budkowski, A.; Steiner, U.; Klein, J.; Schatz, G. *Europhys. Lett.* **1992**, *18*, 705.
(15) Dudowicz, J.; Freed, M. S.; Freed, K. F. *Macromolecules* **1991**, *24*, 5096.
(16) Freed, K. F.; Dudowicz, J. *Theor. Chim. Acta* **1992**, *82*, 357.
(17) Yethiraj, A.; Schweizer, K. S. *J. Chem. Phys.* **1993**, *98*, 9080.
(18) Sariban, A.; Binder, K. *J. Chem. Phys.* **1987**, *86*, 5859.
(19) Sariban, A.; Binder, K. *Macromolecules* **1988**, *21*, 711.
(20) Kumar, S. *Macromolecules* **1994**, *27*, 260.
(21) Tang, H.; Freed, K. F. *J. Chem. Phys.* **1991**, *94*, 1572.
(22) Liu, J.; Deng, Q.; Jean, Y. C. *Macromolecules* **1993**, *26*, 7149.
(23) Sakurai, S.; Jinnai, H.; Hasegawa, H.; Hashimoto, T.; Han, C. C. *Macromolecules* **1991**, *24*, 4839. Hasegawa, H.; Sakurai, S.; Takenaka, M.; Hashimoto, T.; Han, C. C. *Macromolecules* **1991**, *24*, 1813. Sakurai, S.; Hasegawa, H.; Hashimoto, T.; Hargis, I. G.; Aggarwal, S. L.; Han, C. C. *Macromolecules* **1990**, *23*, 451.
(24) *Polymer Handbook*; Brandrup, J., Immergut, E. H., Eds.; Wiley: New York, 1989.
(25) Freed, K. F.; Dudowicz, J. *J. Chem. Phys.* **1992**, *97*, 2105. Dudowicz, J.; Freed, K. F. *Macromolecules* **1993**, *26*, 213.
(26) Dudowicz, J.; Freed, K. F. *J. Chem. Phys.* **1994**, *100*, 4653.
(27) Krishnamoorti, R.; Graessley, W. W.; Balsara, N. P.; Lohse, D. J. *J. Chem. Phys.* **1994**, *100*, 3894.
(28) Jinnai, H.; Hasegawa, H.; Hashimoto, T.; Han, C. C. *Macromolecules* **1992**, *25*, 6078.
(29) Freed, K. F.; Dudowicz, J., unpublished work.
(30) Freed, K. F.; Dudowicz, J. *Macromol. Symp.* **1994**, *78*, 29.
(31) Schweizer, K. S.; Curro, J. G. *J. Chem. Phys.* **1989**, *91*, 5059. Schweizer, K. S. *Macromolecules* **1993**, *26*, 6033.
(32) Tang, H.; Freed, K. F. *Macromolecules* **1991**, *24*, 5112.
(33) Dudowicz, J.; Freed, K. F. *J. Chem. Phys.* **1992**, *96*, 9147.